GAMMA RAY SPECTROSCOPY USING HIGH PURITY GERMANIUM DETECTOR

Jim M John

January 15, 2018

1. Abstract

The characterization of HPGe detector was carried out, followed by spectral analysis of various sources using the HPGe detector. The efficiency and resolution is found out by characterizing the HPGe with ^{152}Eu and ^{54}Mn.
The efficiency of the detector found using ^{152}Eu and ^{54}Mn is utilized to determine the unknown source strength of ^{56}Co.
The studies on neutron irradiated samples of ^{124}Sn and Borated Rubber for the low background studies of TIN.TIN experiment were performed with HPGe and $CeBr_3$. The ^{124}Sn was neutron irradiated at DHRUVA reactor,BARC. Both half-life tracking of 511 KeV line and line identification is performed for borated rubber, which was neutron irradiated with Pelletron Linac Facility, Mumbai (Where the neutrons with a wide energy range are produced by colliding high energy protons with ^{9}Be, ^{9}Be(p,n)^{9}B(Q=-1.850 MeV)).
Also the half life tracking of a spectral line in ^{56}Fe is done, which was also neutron irradiated at Pelletron Linac Facility.

2. Introduction

Among semiconductor detectors, Germanium detectors offers the advantage of having larger stopping power (necessary for gamma ray detection). Initially lithium drifted germanium detectors were made with compensated doping (lithium is drifted from the outer surface of p-type germanium). But the depletion region that can be formed from this normal purity detectors is of the range 2 to 3 mm. The high purity germanium detectors (intrinsic germanium) are made to overcome this disadvantage and this effort bestowed with a depletion region width extending to centimeter regime. The thickness of depletion region is given by

$$d = \left(\frac{2\epsilon V}{eN}\right)^{1/2}$$

where ϵ is the dielectric constant, V is the reverse bias voltage, N is the net impurity concentration in the bulk semiconductor material and e is the electronic charge. For high purity germanium the impurity concentration is approximately 10^{16} atoms/m^3, ϵ is 16.2 at 300 K. From this for an applied voltage of 2.4 KV

$$d = \left(\frac{2\epsilon V}{eN}\right)^{1/2} = \left(\frac{2 \times 16.2 \times 2400}{1.6 \times 10^{-19} \times 10^{16}}\right)^{1/2}$$

2.1 HPGe detector

The germanium detectors is having high energy resolution. In our experiment we have used a *closed-ended coaxial* configuration in which the central core is removed and the outer electrode is extended over the detecting face of the crystal. The rectifying contact (limits the direction of current) is placed on the outer surface such that the high electric field is created near the outer surface. The type of the rectifying contact will depend on the

small fraction of impurities present in the germanium. And the voltage is applied such that the it will form a reverse bias depletion region.
The resolution is determined by the photon statistics (which is poisonian), due to variation in charge collection efficiency at different energies and due to electrical noise. Usually the source is kept at a small distance away from the detector face, such that the simultaneous emission of γ rays will not lead to summing effect.

2.2 HPGe detector experimental setup

we are using coaxial p-type HPGe detector (ORTEC GEM75-95-LB-C-HJ). So the rectifying contact is n^+ and we are applying -ve voltage to the outer surface of the HPGe. The entire setup is cooled to liquid nitrogen temperature to reduce the leakage current. For applying the signal we used a SHV cable(Safe High Voltage). The signal is amplified by a pre-amplifier near HPGe detector, then using a lemo cable the output of pre-amplifier is connected to digitizer (N6724). The digitizer is having two main components, ADC and DPP-PHA (Digital Pulse Processing-Pulse Height Analyzer). The ADC quantize the analog signal and DPP-PHA converts the pulse height information to energy information depending on the gain set by the computer software to interface the digitizer. The specification of the digitizer is mentioned in Table 1.

Table 1: N6724 Specification, Reference : [2]

Number of quantization bits in ADC	14 bit
ADC Frequency	100 MHz
Maximum peak to peak Voltage	2.25 V

The schematic of the experimental setup is shown in Figure 1.

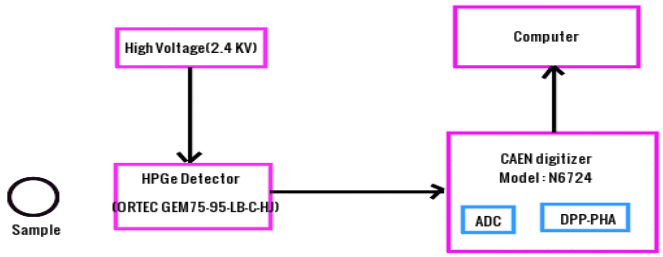

Figure 1: The schematic of the experimental setup.

The data acquisition is done in the computer connected to digitizer, which produce a list file with energy and time stamp. Using a program written in root, we can convert the

list file to energy histogram(eh) file where we bin it properly. Then the .eh file is analyzed using LAMPS(Linux Advanced Multi Parameter System) software.
For a peak to peak pulse of 65.2 mV, we measured a rise time of 280 nS and a fall time of 180 μS using a digital CRO.
The ^{152}Eu, ^{54}Mn and ^{56}Co are counted using D2. These sources are kept at 10 cm away from the detector face to avoid the summing effect. ^{124}Sn is counted with CRADLE(Cryocooled detector for Rare Decay and Low Background Experiment) on face and borated rubber is counted using TILES (Tifr Low Background Experimental Setup) on face. The TILES setup uses HPGe detector shielded by Cu and low activity Pb. Also it uses veto system to reject the rays coming from outside. CRADLE is also shielded by low activity Pb, whereas D2 is not. The HPGe detector in D2 is covered by aluminum, whereas in CRADLE and TILES setup we use HPGe detector covered with carbon fiber. The relative efficiency of D2 and CRADLE is 30%, and that of TILES is 70%. Since the later two are counted on face there will be prominent summing effect.

3. Data Analysis

3.1 HPGe detector

The efficiency of HPGe detector will vary with energy and the source-detector geometry. So before doing experiments with unknown source strength, one has to calibrate the detector for that particular geometry and energy. The bias voltage of the detector is increased to 2.4 KV slowly. We have kept the digitizer in 1 MHz sampling frequency mode and the gain is adjusted such that the required spectral range can be quantized using 8192 levels in ADC.
^{152}Eu and ^{54}Mn is used to find the efficiency of the detector for a geometry where source is placed 10 cm away from the detector face. ^{152}Eu is having many lines such that we can interpolate and perform a fitting for the efficiency with respect to energy. The initial activity of ^{152}Eu is given to be 35928±82 *dps* as on 1^{st} June 2011. The efficiency is estimated using the equation

$$\epsilon = \frac{N_\gamma}{I_\gamma \times t \times \frac{dN}{dt}}$$

where N_γ is the count for time t, I_γ is the branching ratio of that line and $\frac{dN}{dt}$ is the activity at the time of counting. Also the error associated with each data point is found out using error propagation. The fitting is performed with a function of the form

$$\epsilon(E) = p_0 + \frac{p_1}{E} + \frac{p_2}{E^2}$$

where E is the energy and the p_0, p_1 and p_2 are the parameters derived after fitting which is shown in Figure 2a.

Also we have derived the variation resolution with respect to energy using the formula

$$R = \frac{FWHM}{E}$$

The derived relation is plotted in Figure 2b and fitted using the function

$$R = c_0 + \frac{c_1}{\sqrt{E}}$$

The FWHM due to photon statistics is

$$FWHM = 2.35\sqrt{F\epsilon E}$$

Where F is the Fano factor, ϵ is the energy needed to create one electron hole pair(2.96 eV) and E is the gamma ray energy. We have observed a FWHM of 2.5 KeV at 1.3 MeV energy. This gives a Fano factor of 0.3. Since other noise will also lead to the spread, the calculation of Fano factor is not accurate. Compared to the Fano factor(0.08) given in Knoll[3], the calculated value is 4 times high, which means the electronic noise and the charge collection efficiency is contributing to the FWHM a lot.

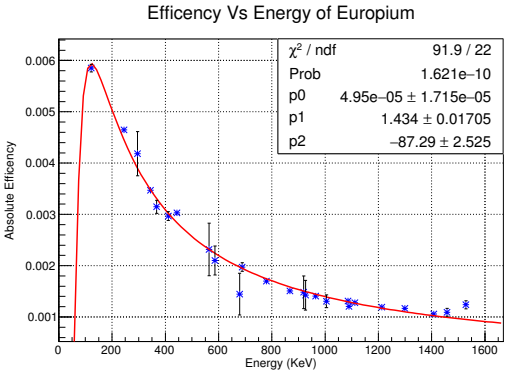

(a)Energy Vs Efficiency plot of the detector

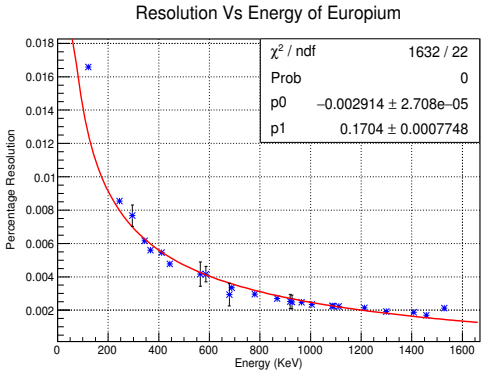

(b)Energy Vs Resolution plot of the detector

The spectrum of ^{152}Eu and ^{54}Mn is shown in Figure 3a and Figure 3b respectively.

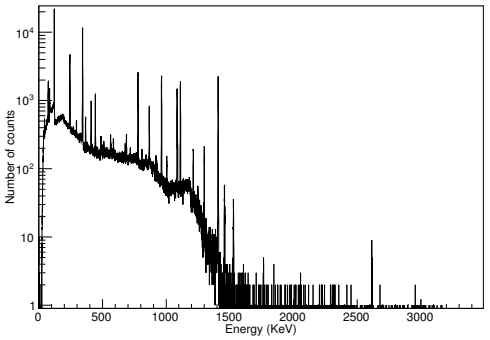

(a)Spectrum of ^{152}Eu

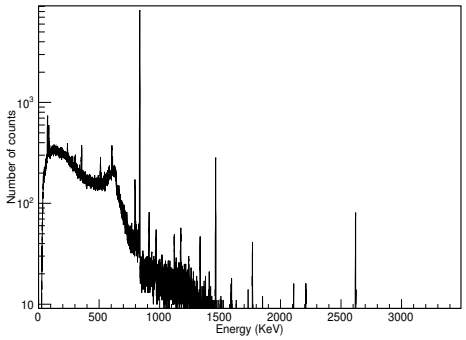

(b)Spectrum of ^{54}Mn

3.2 Estimating unknown source strength of ^{56}Co

The efficiency calculated using the fitting parameters in the Energy Vs Efficiency plot of ^{152}Eu is 0.0016±0.00003 at 848.7 KeV (The small deviation in the value is due to the calibration error in our analysis). Using this efficiency,

$$\text{Source strength of } ^{56}\text{Co} = \frac{N_\gamma}{I_\gamma \times t \times \epsilon} = 2343 \pm 45 \; dps$$

The unknown source strength of ^{56}Co is derived independently with the help of efficiency obtained using ^{54}Mn. The initial activity of ^{54}Mn is given to be 3600±71 *dps* as on 28^{th} January 2016. The ^{54}Mn is having a line near to the line from the parent ^{56}Co (846.77 KeV).

The efficiency calculated from the ^{54}Mn analysis at energy 836.7 keV is 0.0017±0.00004. Using this efficiency,

$$\text{Source strength of } ^{56}\text{Co} = \frac{N_\gamma}{I_\gamma \times t \times \epsilon} = 2181 \pm 52 \; dps$$

The spectrum of ^{56}Co is shown in Figure 4

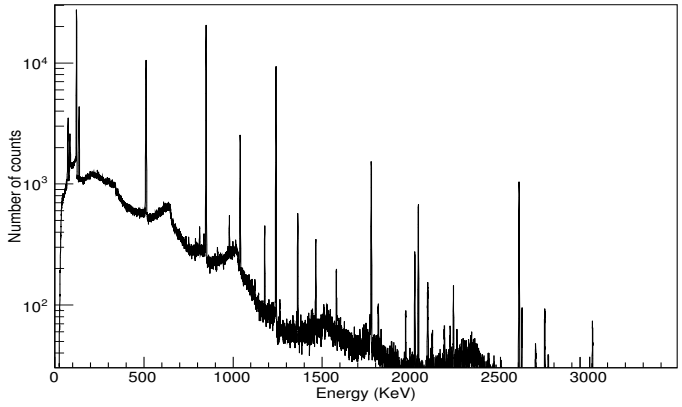

Figure 4: The spectrum of ^{56}Co

Table 2: Source strength of ^{56}Co

	Percentage Efficiency at 848.7 KeV	Estimated source strength of ^{56}Co
^{152}Eu	0.0016±0.00003	2343±45 *dps*
^{54}Mn	0.0017±0.00004	2181±52 *dps*

3.3 Spectral analysis of neutron irradiated ^{124}Sn

The neutron irradiated 99.26% enriched ^{124}Sn is counted using CRADLE. The source was placed on face of the detector. The corresponding source and decay chain is found from NNDC [1].

Energy	Energy from NNDC	Source	Decay Mode
176.4	176.3	^{125}Sb (7/2+)	β^{-1}
332.1	332.1	^{125}Sn (3/2+)	β^{-1}
351.7	350.9	^{125}Sn (11/2-)	β^{-1}
380.6	380.5	^{125}Sb (7/2+)	β^{-1}
428.1	427.9	^{125}Sb (7/2+)	β^{-1}
463.5	463.4	^{125}Sb (7/2+)	β^{-1}
470.2	469.9	^{125}Sn (11/2-)	β^{-1}
511.1	511	BG	
583.5	583	^{208}Tl (5+)	β^{-1}
600.9	600.6	^{125}Sb (7/2+)	β^{-1}
607.0	606.7	^{125}Sb (7/2+)	β^{-1}
636.2	635.9	^{125}Sb (7/2+)	β^{-1}
671.8	671.4	^{125}Sb (7/2+)	β^{-1}
800.5	800.3	^{125}Sn (11/2-)	β^{-1}
822.8	822.5	^{125}Sn (11/2-)	β^{-1}
893.6	893.4	^{125}Sn (11/2-)	β^{-1}
911.4	912.0	^{125}Sn (11/2-)	β^{-1}
915.9	915.6	^{125}Sn (11/2-)	β^{-1}
935.0	934.6	^{125}Sn (11/2-)	β^{-1}
1017.9	1017.4	^{125}Sn (11/2-)	β^{-1}
1067.5	1067.1	^{125}Sn (11/2-)	β^{-1}
1089.5	1089.2	^{125}Sn (11/2-)	β^{-1}
1120.6	1120.0	^{214}Bi (1-)	β^{-1}
1420.2	1419.7	^{125}Sn (11/2-)	β^{-1}
1460.9	1460.0	^{40}K	ϵ
1731.9	1731.0	IInd escape of ^{24}Na	
2002.0	2002.1	^{125}Sn (11/2-)	β^{-1}
2242.5	2242.0	Ist escape of ^{24}Na	
2276.3	2275.7	^{125}Sn (11/2-)	β^{-1}
2613.9	2614.5	^{208}Tl (5+)	β^{-1}
2753.3	2754.0	^{24}Na	β^{-1}

3.4 Half-life tracking of a spectral line from ^{56}Fe

To get exposure to the half-life tracking of spectral lines, we have done the tracking of an unknown line in ^{5}6Fe with energy 847±0.1 KeV. The source was counted for 2 Hrs using HPGe Detector. We need to observe the source for a time comparable to the half-life of

the interested line. The file is split into several files using root. We obtained files with 10 minutes, 15 minutes and 20 minutes splitting. Then the number of un-decayed nucleus is fitted with the exponential

$$N = N_0 e^{-\lambda t}$$

and is shown in Figure 5

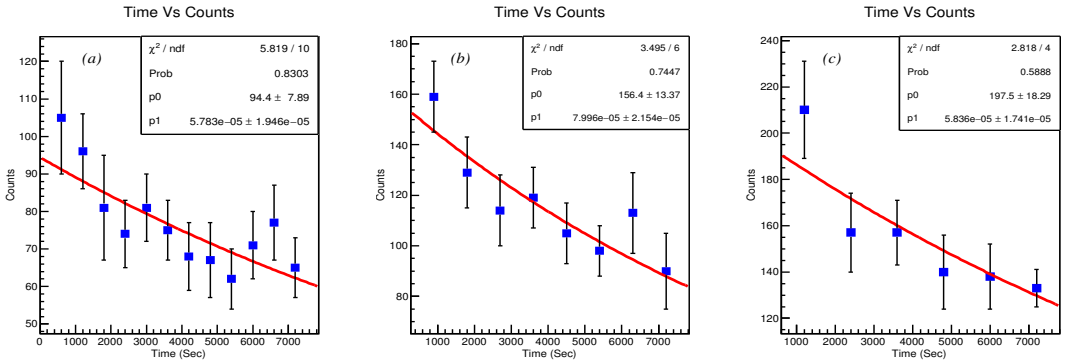

Figure 5: ^{56}Fe half-life tracking (a)Decay with counts integrated to 10 mins (b)Decay with counts integrated to 15 mins (c)Decay with counts integrated to 20 mins.

The observed half-life values are
(a) Half-life corresponding to 10 mins split = 3.32±1.1 hrs
(b) Half-life corresponding to 15 mins split = 2.43±0.66 hrs
(c) Half-life corresponding to 20 mins split = 3.3±0.96 hrs

3.5 Half-life tracking of 511 line from borated rubber

The half life tracking of 511 KeV line in Borated rubber is performed similar to the half life tracking described in Section 3.4. Since the peak was prominent we counted it using $CeBr_3$ for 12 hours. The file was splitted into 50 files with a counting time of 15 minutes each. The graph of undecayed nucleus vs time is fitted with an exponential as shown in Figure 6. The half-life is derived using the fitting parameters.

Derived half-life of 511 KeV line is 12.66±0.102 hours.
The perfect exponential decay curve implies the 511 KeV line is coming form a single type of nucleus.

3.6 Line identification in borated rubber with the help of NNDC [1]

The main objective of half-life tracking of annihilation peak in borated rubber is to identify the prominent impurity (because the 511 KeV line was prominent) (Refer Figure7). We set the half-life range to be compatible with the derived one in Section 3.5 and probable

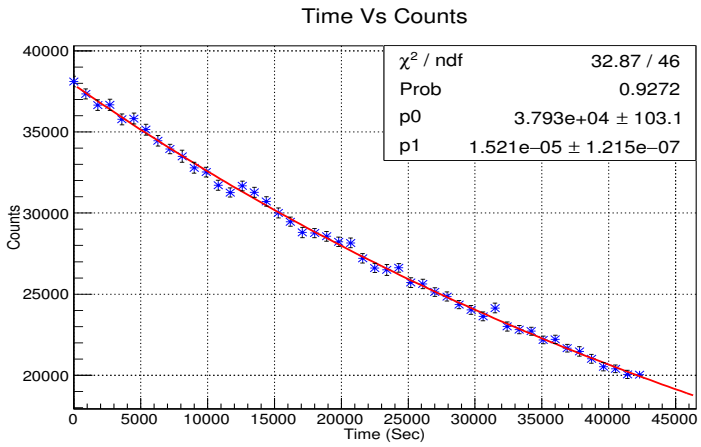

Figure 6: Borated Rubber decay with counts integrated to 15 minutes

impurities was obtained from NNDC [1]. Also the probable reactions are selected by checking the neutron reaction cross-sections in NNDC [1] (sigma portal). DHRUVA produces thermal neutrons(0-10 MeV), while Pelletron Linac Facility produces fast neutrons having energy upto 18 MeV.
It is understood from manufacture specification that, the rubber is borated with the help of some zinc and boron compounds. Also the half life obtained from line tracking is same as the half-life of ^{64}Cu, which is formed from zinc on neutron irradiation. The half life of ^{64}Cu is 12.701 hours. The 511 KeV line is coming due to the ϵ capture of ^{64}Cu nucleus produced due to neutron irradiation on Zn. This perfectly matches with the observation on Section 3.5. The stable zinc nucleus configurations are ^{64}Zn(49%), ^{66}Zn(27%), ^{67}Zn(4%), ^{68}Zn(18%) and ^{70}Zn(0.4%).

The following are the most probable reaction channels due to neutron irradiation.

$$ {}^{A}_{Z}\mathrm{N}\ (n,\gamma)\ {}^{A+1}_{Z}\mathrm{N} $$

$$ {}^{A}_{Z}\mathrm{N}\ (n,p)\ {}^{A}_{Z-1}\mathrm{N} $$

$$ {}^{A}_{Z}\mathrm{N}\ (n,2n)\ {}^{A-1}_{Z}\mathrm{N} $$

$$ {}^{A}_{Z}\mathrm{N}\ (n,\alpha)\ {}^{A-3}_{Z-2}\mathrm{N} $$

The reaction channels in Table 3 is derived based on the above probable channels.
The results are confirmed by taking the ratio of number of counts in lines from same source and equating it to the theoretical ratio calculated from the branching ratio.

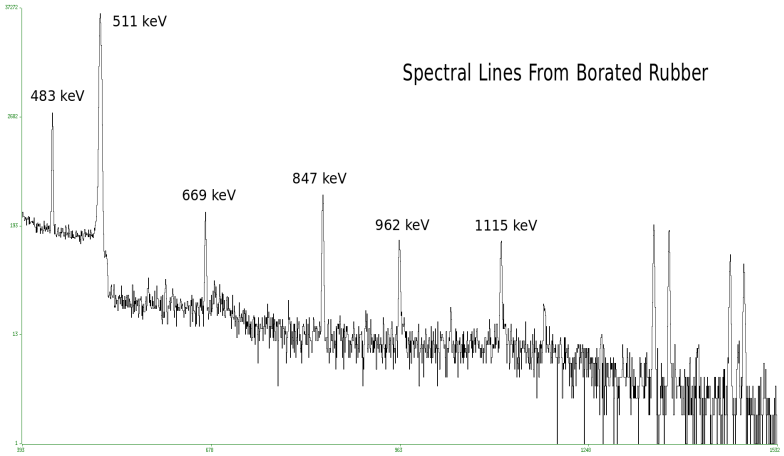

Figure 7: Spectrum of Borated Rubber

The efficiency of the detector at each energy is found using the fitting parameters derived in Section 3.1.

$$\epsilon(E) = p_0 + \frac{p_1}{E} + \frac{p_2}{E^2} = \frac{1.43 \pm 0.02}{E(inKeV)}$$

Equating activity of the two lines, since both are form same source.

$$\frac{N_1}{N_2} = \frac{I_{\gamma 1} \times \epsilon_{\gamma 1}}{I_{\gamma 2} \times \epsilon_{\gamma 2}}$$

[Note :-The error in ϵ (0.02) is prominent (Error in energy = 0.014 × E)]

- Both 511 KeV line and 1345.98 KeV line are produced in the decay of ^{64}Cu. They have the branching ratio 35.2% and 0.475% respectively.

$$\frac{N_{511}}{N_{1345}} = \frac{142818 \pm 1848}{721 \pm 41} = \frac{35.2 \times 1345.98 \pm 19}{0.475 \times 511.15 \pm 7} \implies 198 \pm 12 \approx 195 \pm 4$$

- Both 846 KeV line and 1810 KeV line are produced in the decay of ^{56}Mn. They have the branching ratio 98.85% and 26.9% respectively.

$$\frac{N_{846}}{N_{1810}} = \frac{1238 \pm 47}{142 \pm 16} = \frac{98.85 \times 1810.79 \pm 25}{26.9 \times 846.86 \pm 12} \implies 8.72 \pm 1.03 \approx 7.85 \pm 0.16$$

- Both 1368 KeV line and 2753 KeV line are produced in the decay of ^{24}Na. They have the branching ratio 99.99% and 99.85% respectively.

$$\frac{N_{1368}}{N_{2753}} = \frac{639 \pm 32}{357 \pm 28} = \frac{99.99 \times 2753.04 \pm 39}{99.85 \times 1368 \pm 19} \implies 1.79 \pm 0.2 \approx 1.2 \pm 0.02$$

The pulser is adjusted to 10 Hz. Therefore for a counting time of 1516 sec, we should observe 15160 counts at 2933 KeV. Which exactly matches with the observed area under the curve at 2933 KeV (15002±128).

Energy	Counts	Source	Decay Chain	Reaction Channel
438.83	7811±167	^{68}Zn, ^{70}Zn	^{69}Zn	(n,γ) , (n,2n)
511.15	142818±1848	^{64}Zn	^{64}Cu	(n,p)
669.97	701±46	^{64}Zn	^{63}Zn	(n,2n)
846.86	1238±47	^{56}Fe	^{56}Mn	(n,p)
962.43	433±35	^{64}Zn	^{63}Zn	(n,2n)
1115.66	431±39	^{64}Zn, ^{66}Zn	^{65}Zn	(n,γ),(n,2n)
1180.78	106±21	(669+511) summing	^{63}Zn (Not Sure)	
1345.98	721±41	^{64}Zn	^{64}Cu	(n,p)
1368.84	639±32	^{23}Na or ^{27}Al	^{24}Na	
1460.86	341±27	^{40}K	^{40}K	
1481.95	227±23	^{58}Fe	^{59}Fe	(n,γ)
1810.79	142±16	^{56}Fe	^{56}Mn	(n,p)
2112.88	80±13	^{56}Fe	^{56}Mn	(n,p)
2243.20	48±12		I^{st} Escape of ^{24}Na	
2613.59	51±12	^{232}Th	^{208}Tl	
2753.05	357±28	^{23}Na or ^{27}Al	^{24}Na	
2933.06	15002±128	Pulser		

Table 3: Reaction Channel of lines from borated rubber

4. Results And Conclusion

HPGe detector is characterized. The variation of resolution and efficiency with respect to incident gamma energy is found. The source strength of ^{56}Co is found to be ~2343±45 *dps*. Line identification of neutron irradiated 99.26% enriched tin is carried out. The half-life tracking of 847 KeV line from ^{56}Fe and 511 KeV line from borated rubber is done. This procedure resulted a 3±1 hours half life for 847 KeV line from ^{56}Fe and 12.66±0.102 hours for 511 KeV line form borated rubber. The source of lines from neutron irradiated borated rubber is found to be Zinc and Iron. But the channel which populate ^{24}Na is unknown.

References

[1] National Nuclear Data Center. NNDC https://http://www.nndc.bnl.gov/, 2017.

[2] CAEN Electronic Instrumentation. N6724 http://www.caen.it/csite/CaenProd.jsp?idmod=626&parent=12#, 2018.

[3] Glenn F. Knoll. Radiation detection and measurement. Edition 4:Pages 857, 1979.